Journal of Environmental Management 321 (2022) 115965

Contents lists available at ScienceDirect

Journal of Environmental Management

journal homepage: www.elsevier.com/locate/jenvman

Research article

Removal of nitrate and pesticides from groundwater by nano zero-valent iron injection pulses under biostimulation and bioaugmentation scenarios in continuous-flow packed soil columns

Oriol Gibert [a,b,*], Damián Sánchez [c], José Luis Cortina [a,b,d]

[a] Chemical Engineering Department, EEBE, Universitat Politècnica de Catalunya (UPC)-BarcelonaTech, c/Eduard Maristany 10-14, Barcelona, 08019, Spain
[b] Barcelona Research Center in Multiscale Science and Engineering, EEBE, Universitat Politècnica de Catalunya (UPC)-BarcelonaTech, c/Eduard Maristany 10-14, Barcelona, 08019, Spain
[c] Cetaqua-Water Technology Centre, c/ Severo Ochoa 7, 29590, Málaga, Spain
[d] Cetaqua-Water Technology Centre, Carretera d'Esplugues 75, 08940, Cornellà de Llobregat, Spain

ARTICLE INFO

Keywords:
Denitrification
Abiotic chemical nitrate reduction
Nano zero-valent iron
Injection pulse
Column experiments
Pesticides

ABSTRACT

This study evaluates the NO_3^- removal from groundwater through Heterotrophic Denitrification (HDN) (promoted by the addition of acetate and/or an inoculum rich in denitrifiers) and Abiotic Chemical Nitrate Reduction (ACNR) (promoted by pulse injection of zerovalent iron nanoparticles (nZVI)). HDN and ACNR were applied, separately or combined, in packed soil column experiments to complement the scarce research on pulse-injected nZVI in continuous-flow systems mimicking a Well-based Denitrification Barrier. Together with NO_3^-, the removal of two common pesticides (dieldrin and lindane) was evaluated. Results showed that total NO_3^- removal (>97%) could be achieved by either bioestimulation with acetate (converting NO_3^- to N_2(g) via HDN) or by injecting nZVI (removing NO_3^- via ACNR). In the presence of nZVI, NO_3^- was partially converted to N_2(g) and to a lower extent NO_2^-, with unreacted NO_3^- being likely adsorbed onto Fe-(oxy)hydroxides. Combination of both HDN and ACNR resulted in even a higher NO_3^- removal (>99%). Interestingly, nZVI did not seem to pose any toxic effect on denitrifiers. These results showed that both processes can be alterned or combined to take advantage of the benefits of each individual process while overcoming their disadvantages if applied alone. With regard to the target pesticides, the removal was high for dieldrin (>93%) and moderate for lindane (38%), and it was not due to biodegradation but to adsorption onto soil. When nZVI was applied, the removal increased (generally >91%) due to chemical degradation by nZVI and/or adsorption onto formed Fe-(oxy)hydroxides.

1. Introduction

In-situ treatment of groundwater contaminated by nitrate (NO_3^-) and pesticides has attracted a growing interest in the field of environmental remediation. One of the most cost-effective methods to remove NO_3^- from water on a large scale is Heterotrophic Denitrification (HDN), whereby denitrifying microbes use NO_3^- as terminal electron acceptor (which is sequentially reduced to intermediates NO_2^-, NO(g), N_2O(g), and ultimately to harmless nitrogen gas N_2(g)) and an organic substance as electron donor and energy source (Greenan et al., 2006; Richa et al., 2022) as described by reaction 1 (Robertson et al., 2008):

$$4\ NO_3^- + 5\ CH_2O \rightarrow 2\ N_2(g) + 5\ HCO_3^- + 2\ H_2O + H^+ \quad (1)$$

where CH_2O represents a generic biodegradable organic compound. This can be of a wide variety of forms, from insoluble natural lignocellulosic materials (such as woodchips, straws, reeds, cotton, or agricultural wastes) to more or less purified low-molecular-weight liquid organic compounds (such as methanol, ethanol, acetate, or glucose) (Calderer et al., 2010; Costa et al., 2018). More recently, some synthetic polymers (such as polybutylene succinate (PBS), or polyacrylic acid (PAA), among others) have been reported to have potential as alternative providers of organic carbon for HDN (Pang and Wang, 2021).

However, while denitrifying bacteria are ubiquitous in nature (and therefore expected also in aquifers), labile CH_2O is rarely present in subsurface environments at sufficiently high contents to promote HDN (Greenan et al., 2006). One technology developed for supplying organic

* Corresponding author. Chemical Engineering Department, EEBE, Universitat Politècnica de Catalunya (UPC)-BarcelonaTech, c/Eduard Maristany 10-14, Barcelona, 08019, Spain.
E-mail address: oriol.gibert@upc.edu (O. Gibert).

https://doi.org/10.1016/j.jenvman.2022.115965
Received 25 May 2022; Received in revised form 27 July 2022; Accepted 4 August 2022
Available online 15 August 2022
0301-4797/© 2022 The Authors. Published by Elsevier Ltd. This is an open access article under the CC BY-NC license (http://creativecommons.org/licenses/by-nc/4.0/).

carbon into the aquifer (i.e. under a biostimulation scheme) is the Well-based Denitrification Barriers (WDBs), in which soluble organic compounds are introduced as aqueous solutions from the surface into the aquifer through injection wells (Margalef-Marti et al., 2019; Han et al., 2020). Alternatively, denitrifying microorganisms may also be introduced (i.e. under a bioagumentation scheme) in order to enhance HDN (Anderson et al., 2020). HDN has some drawbacks though: the denitrification rate can be relatively slow, especially in cold temperature (Anderson et al., 2020), and the external organics input can cause secondary contamination (e.g. excessive release of DOC and/or NH_4^+, excessive production of biomass, generation of undesirable gases such as CH_4 and N_2O …) (Gibert et al., 2008; Hwang et al., 2011; Burbery et al., 2022).

An alternative for reducing NO_3^- is through Abiotic Chemical Nitrate Reduction (ACNR) with zero valent iron (ZVI or Fe^0) via the redox reactions 2a and 2b (Yang and Lee, 2005):

$$NO_3^- + 4\ Fe^0(s) + 7\ H_2O \rightarrow NH_4^+ + 4\ Fe^{2+} + 10\ OH^- \quad (2a)$$

$$2\ NO_3^- + 5\ Fe^0(s) + 6\ H_2O \rightarrow N_2(g) + 5\ Fe^{2+} + 12\ OH^- \quad (2b)$$

ZVI is a highly reactive and excellent electron donor, and among the advantages of ACNR over HDN are the stronger reduction performance also at low temperature, the faster kinetics of the reaction, the lower biomass formation, and the lack of risk of secondary organic carbon contamination (Araújo et al., 2016; Liu and Wang, 2019). ZVI for in-situ treatment of groundwater has traditionally relied on millimetric ZVI (mmZVI), particularly as solid filling material in PRBs (alone or together with a solid organic substrate) for a wide variety of contaminants, including halogenated organic compounds (Yabusaki et al., 2001; Grau-Martínez et al., 2019), heavy metals and metalloids (Ludwig et al., 2009; Gibert et al., 2013), and radionuclides as U(VI) species (Gu et al., 2002). Removal of NO_3^- has been observed in some of these field mmZVI-bearing PRBs.

But research on ZVI for in-situ remediation has experienced a boost since its synthesis as micro-sized (mZVI) and especially nano-sized ZVI (nZVI) (Liu and Wang, 2019; Zhou et al., 2022). The reason is that nZVI is more reactive in comparison to mmZVI and mZVI (thanks to the small particle size and large surface of nZVI) at the same time that nZVI, similarly to mZVI, can be injected in the form of aqueous suspension directly into the contaminated aquifers (Araújo et al., 2016; Jiang et al., 2018). Nevertheless, bare nZVI presents two important weaknesses: nZVI particles tend to agglomerate and become passivated rapidly in water (Araújo et al., 2016; Liu and Wang, 2019). These weaknesses can be mitigated by coating nZVI with appropriate polymers that can enhance the stability and dispersion of nZVI and, on the other hand, protect nZVI against oxidation (Peng et al., 2019). If biodegradable, these polymers can potentially act as a carbon source and promote HDN.

An issue that arises concerns regarding ACNR is what end-product results from ZVI-mediated ACNR. A number of published studies report NH_4^+ as the major end-product as shown in reaction 2a (Westerhoff and James, 2003; Hwang et al., 2011), while others indicate that, when nZVI is used instead of mZVI, the major product is $N_2(g)$ according to reaction 2b (Choe et al., 2000; Chen et al., 2005; Zhang et al., 2010a; Hosseini and Tosco, 2015). Lying between these two extremes, other studies report that nearly all possible forms of N by-products, mainly NO_2^-, $N_2(g)$, and $NH_4^+/NH_3(g)$ (in varying proportions) can form, also when using nZVI, depending on the reaction conditions (Yang and Lee, 2005; Zhang et al., 2010b; Hosseini et al., 2018; Grau-Martínez et al., 2019).

Further efforts have explored the combination of HDN and ZVI-mediated ACNR for the removal of NO_3^- from water. Confronting findings are reported on this issue. On the one hand, enhanced NO_3^- removal has been reported when coupling organic substrates (maize cobs, beech sawdust, cotton, pine bark) with ZVI (Huang et al., 2015; Hosseini and Tosco, 2015). Besides promoting ACNR, ZVI in these systems may favour the removal of NO_3^- by providing reducing conditions required by heterotrophic denitrifiers (Liu et al., 2013) and, according to some published works, providing H_2, which would allow the development of hydrogen-based autotrophic denitrification (ADN) (Gu et al., 2002; Grau-Martínez et al., 2019), while some others have not observed this effect (Ma et al., 2015; Wu et al., 2013). The oxidation of ZVI and subsequent reduction of NO_3^- is described by reactions 3 and 4 (Pang and Wang, 2021):

$$Fe^0(s) + 2\ H_2O \rightarrow Fe^{2+} + H_2(g) + 2\ OH^- \quad (3)$$

$$2\ NO_3^- + 5\ H_2(g) \rightarrow N_2(g) + 4H_2O + 2OH^- \quad (4)$$

One the other hand, other studies have noticed that nZVI (and more particularly Fe^{2+} generated from ZVI oxidation) may exhert a toxic effect on microorganisms (Jiang et al., 2018; Cojean et al., 2020), and that this toxic effect may be attenuated if stabilized-nZVI is used instead of bare-nZVI (Wang et al., 2014). Whether the overall effect of combining HDN and nZVI-assisted ACNR is beneficial or harmful in removing NO_3^- remains poorly understood.

Despite the dynamic nature of field-scale WDB systems and the acknowledgement that nZVI performance is dependent on its mobility, only few laboratory studies have been conducted on continuous-flow systems (columns or bench-scale aquifer models) so far. Of them, most have assessed the effect of ZVI (mZVI or nZVI) immobilized within the filling material (commonly aquifer soil) (Westerhoff and James, 2003; Kim et al., 2012; Hosseini et al., 2018; Shubair et al., 2018), sometimes mixed with a natural organic solid organic substrate (Hosseini and Tosco, 2015; Huang et al., 2015). However, such setups might be more representative of a PRB than of a WDB. Studies on column nZVI pulse injection for NO_3^- removal are scarce. Hosseini et al. (2011) investigated the application of bare nZVI/Cu pulse injections into a packed sand column to remove NO_3^- from groundwater under different conditions of nZVI/Cu dosages, NO_3^- concentrations and pore water velocities through the columns, but focusing only on ACNR without considering HDN. In a previous study we evaluated the effect of nZVI stabilized with an organic polymer (PAA) and pulse-injected into packed sand columns at a dosage of 10 g nZVI/L and under different influent NO_3^- concentrations and without supplementation of any other organic substrate other than the stabilizer PAA. Results showed that PAA did not enhance HDN and that NO_3^- was removed basically through nZVI-assisted ACNR (Gibert et al., 2022).

Furthermore, it has been reported that nZVI has potential to remove also pesticides (Elliott et al., 2009; Gusain et al., 2019), which often coexist with NO_3^- in groundwater affected by agricultural pollution. Removal of pesticides from groundwater has been investigated through physical, chemical, and biological processes with different degrees of success. Some of them (e.g. tight membrane filtration, photocatalytic degradation …) can only be applied in ex-situ treatments and/or are very costly, making them unfeasible for field-scale in-situ applications, while some others (e.g. adsorption) are not always effective at removing pesticides. Biodegradation of pesticides has also been researched, but some pesticides are recalcitrant and, if eventually biodegraded, the process may take too long and can be unpredictable (Marican and Durán-Lara, 2018; Hassanpour et al., 2019). Clearly, other approaches are needed. As mentioned above, oxidation by nZVI appears as a promising alternative.

However, again as with the removal of NO_3^- by ZVI, most published studies have been performed on batch mode (Elliott et al., 2009; Graça et al., 2020), and the scarce column experiments have applied ZVI as filling material, usually combined with sand, representing a PRB (Dominguez et al., 2016; Abbas et al., 2021). These studies have demonstrated that pesticides lindane, endrin, dieldrin and DDT were removed by >94% during the first 13 days, but this percentage decreased for some pesticides in the following 12 days to 88% (Abbas et al., 2021). In another study, El-Temsah et al. (2013) performed column experiments during which a nZVI suspension was added drop-wise from the top with a pipette, resembling a WDB system, for the evaluation

of nZVI potential in degrading pesticide DDT. Addition of nZVI led to degradation of 45% of the entering DDT. Considering these promising results, the potential of nZVI in reducing pesticides in WDB systems clearly needs to be explored.

Within this framework, there is a need of studies exploring the combination of HDN and nZVI-mediated ACNR in continuous-flow systems where nZVI is pulse injected for the simultaneous removal of NO_3^- and pesticides. This combination may have the potential of overcoming the drawbacks posed by HDN or ACNR alone (e.g. excessive formation of biomass, slowness of NO_3^- removal, formation of undesirable NO_2^- and NH_4^+ …) and even enhancing HDN due to oxygen capturing performance of nZVI (as oxygen may compete with NO_3^- as electron acceptor) and the achievement of more reducing conditions required by denitrifiers. On the other hand, however, it also needs to be assessed whether Fe^{2+} ions exhert any toxic effect on denitrifiers and hinder HDN. An additional potential advantage of this approach is the removal of those pesticides resistant to biodegradation but prone to be adsorbed on Fe-(oxy)hydroxides formed on nZVI particles. These hypotheses constitute the basis of the present study.

The objectives of this study in continuous flow packed columns were 1) to evaluate the effect of biostimulation (by the addition of acetate), bioaugmentation (by the addition of an inoculum), and pulse-injection of polymer-coated nZVI (separately or combined) on the removal of NO_3^- from contaminated groundwater; 2) to determine the removal of two pesticides (dieldrin and lindane) under the mentioned scenarios; and 3) to quantify the densities of two main genes involved in HDN (*nirS* and *nirK*).

2. Materials and methods

2.1. Materials

Soil and groundwater samples were collected from the aquifer of La Vega Media y Baja of the Segura river (Murcia, SE Spain). Soil mainly consisted of medium to coarse gravel and sand, and groundwater presented the composition shown in Table 1. Groundwater was refrigerated at 4 °C until use in the laboratory. Since groundwater revealed a relatively low concentration of NO_3^- (24.2 mg/L), it was artificially spiked with NO_3^- to achieve a final concentration of 100 mg/L. This increase in NO_3^- was not expected to change much the overall system performance. In fact, published studies on column experiments report similar NO_3^- removal percentages (of 65%, 58%, and 67%, as measured at the exit of the column) when influent nitrate concentration was increased from 100 mg/L to 200 mg/L and 300 mg/L, respectively, while maintaining the rest of parameters investigated (nZVI dose, pore water velocity) constant (Hosseini et al., 2011). It is also worthnoting from Table 1 that, as it is the case in many aquifers, the content of TOC was low (<1.0 mg/L), and therefore HDN was not expected to be supported unless a labile organic compound was externally supplied.

Table 1
Composition of the groundwater collected at the aquifer of La Vega Media y Baja of the Segura river used for this study (values are average of three analyses).

Parameter	Units	Concentration
pH		7.8 ± 0.2
Cond	(μS/cm)	2412 ± 78
NO_3^-	(mg/L)	24.2 ± 0.3
NO_2^-	(mg/L)	<0.05
NH_4^+	(mg/L)	<1
TOC	(mg/L)	<1
SO_4^{2-}	(mg/L)	646.7 ± 7.1
Cl^-	(mg/L)	371.9 ± 4.0
HCO_3^-	(mg/L)	401.3 ± 7.3
PO_4^{3-}	(mg/L)	<4.5
Na^+	(mg/L)	151.2 ± 1.6
K^+	(mg/L)	4.8 ± 0.2
Ca^{2+}	(mg/L)	308.5 ± 4.6
Mg^{2+}	(mg/L)	82.7 ± 2.5
Fe^{2+}	(mg/L)	<0.5

The nZVI particles (Nanofer 25S) were supplied by NANOIRON (Prague, Czech Republic) as a blackish slurry containing water (74.1% (w/w)), Fe^0 (15% (w/w)), Fe_3O_4 (3.5% (w/w)), and Tween 80 (7.4% (w/w)) (according to the manufacturer), the latter being an organic polymer (polysorbate) used as a stabilizer of the nZVI. The capability of Tween 80 in stabilizing nZVI in suspension and thus enhancing its mobility has been reported (Peng et al., 2019). At a content of 7.4%, Tween 80 would represent, if dissolved, an abundant source of organic carbon. One of the objectives of this study was to determine whether this polymer was degradable enough to contribute to HDN. FESEM-EDS analysis of the dried nZVI particles showed a relatively homogeneous solid with agglomerated particles (Fig. 1a) with Fe and O as major elements coming from the Fe^0 core and the shell made of Fe_3O_4(s) or other Fe-(oxy)hydroxides (Fig. 1b). A minor peak of C was also observed coming from the Tween 80 polymer layer coat.

Activated sludge used to inoculate some columns of the study was collected from the secondary treatment of the municipal wastewater treatment plant of El Prat de Llobregat (Barcelona, NE Spain). The sludge consisted of green-gray suspended granules with a volatile suspended solids (VSS) content of 3000 mg/L. After adding a moderate concentration of NO_3^- (approx. 30 mg/L), the fresh sludge was left to sit for two weeks to let organic matter be consumed by microorganisms. Depletion of original organic matter from the sludge was deemed convenient to better monitor the effect of later acetate addition on biological activity.

2.2. Columns experiments design

Five identical columns were filled with the same aquifer soil and fed with the same groundwater (spiked at a NO_3^- concentration of 100 mg/L) but operated under different conditions:

Column A: filled with soil, fed with groundwater, and receiving a pulse of nZVI after 48 days of experiment.

Column B: filled with soil and fed with groundwater supplemented with 100 mg/L acetate (biostimulation).

Column C: filled with inoculated soil (bioaugmentation) and fed with groundwater supplemented with 100 mg/L acetate (biostimulation).

Column D: filled with soil, fed with groundwater, and receiving a pulse of nZVI on day 48. After the pulse of nZVI, groundwater was supplemented with 100 mg/L acetate (biostimulation).

Column E: filled with inoculated soil (bioaugmentation), fed with water supplemented with 100 mg/L acetate (biostimulation), and receiving a pulse of nZVI on day 48.

Fig. 2 shows a scheme of the operation conditions of each aquifer soil containing column:

2.3. Packed soil columns set-up and operation

Continuous-flow experiments were performed in homemade packed-bed columns, each consisting of a transparent methacrylate cylinder (L = 50 cm, i.d. = 5 cm) provided with connectors and valves to allow and control upward passage of groundwater. A metallic mesh disc was placed on the bottom of each column to support the packing soil and prevent material losses. A 4-cm layer of gravel and coarse sand (also from the aquifer) was packed above the disc to ensure a uniform flow through the soil and reduce risk of clogging. Then, each column was packed with 1.3 kg of aquifer soil carefully placed on the gravel and sand layer. The columns were covered with aluminium foil to simulate light conditions within the aquifer. The porosity of the filling material was first estimated by weighing a given mass of soil before and after water saturation and quantified to be approx. 0.20 (which was later experimentally confirmed by a tracer test). Before pumping any water through the columns, they were flushed with pressurized N_2(g) to evacuate air from the soil pores to obtain realistic anaerobic conditions within the

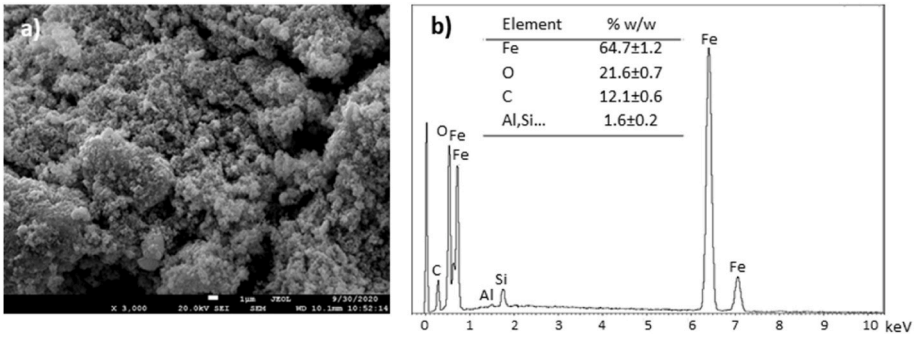

Fig. 1. a) FESEM analysis and b) EDS analysis of the nZVI particles used in this study.

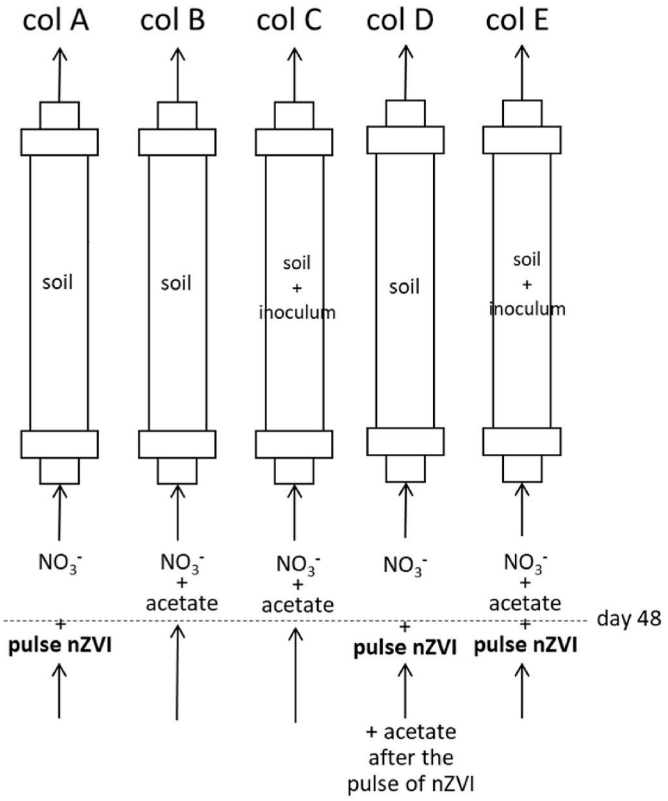

Fig. 2. Scheme of the conditions of each of the five (A, B, C, D, E) aquifer soil containing columns operated in this study.

columns.

Then the columns were fed with deionized water using a mulitport peristaltic pump (Dinko 25 VCF) in an up-flow mode to remove fines from the column and adjust the flow rate to 0.80 mL/min, which was selected to provide a pore water velocity similar to the one observed in the aquifer of La Vega Media y Baja (0.20 cm/min). Taking into account the column volume and the soil porosity, this flow rate resulted in an average hydraulic residence time of 4.9 h. Once the flow rate was adjusted, deionized water (for Columns A, B, and D) or inoculum (with recirculation) (for Columns C and E) was passed over additional 48 h. After this inoculation period, the columns were started to treat groundwater (moment that was considered as the initial time of the experiment). The containers with feed groundwater were purged with N_2(g) to remove any oxygen prior to injection into the column. Columns were left to adapt to this water for a long period of time (48 days) to ensure a good acclimatisation of denitrifying microorganisms to the conditions of each column and achievement of steady-state conditions (evidenced by constant composition in effluent samples). Start-up periods of a few months in order to adapt heterotrophic bacteria to the media are common in column experiments (Banzhaf et al., 2012; Capodici et al., 2018).

On day 40, prior to the injection of nZVI, pesticides dieldrin and lindane were added to feed groundwater (at concentrations around 1.5 μg/L and 3.0 μg/L, respectively) and continuously entered Columns A, B, and E until the end of the experiment. Their choice was based on previous campaigns on the site that revealed these pesticides as the more frequent ones found at highest concentrations.

On day 48, the pulse of nZVI was applied. For this purpose, 3.12 L of nZVI suspension with a content of 3 g nZVI/L (prepared in a separate bottle by dilution of the commercial slurry in deionized water) were injected to Columns A, D, and E at a flow rate of 2.63 mL/min for 6.6 h. This injection was done while maintaining the groundwater flow through the columns to better simulate a field-scale injection in the aquifer. The simultaneous injection of feed groundwater and nZVI into the columns was achieved by means of a T valve installed at the inlet of the columns. Taking into account the flow rates of both inputs and the resulting dilution, the content of nZVI entering the columns was quantified to be 2.3 g nZVI/L (expressed on a bare nZVI basis (i.e. without polymer)). This value was within the range of nZVI doses typically applied for NO_3^- removal (0.5–10 g/L) (Zhang et al., 2010a; Hosseini et al., 2011; Kim et al., 2012; Hosseini and Tosco, 2015). Prior to and during the whole pulse, the nZVI suspension in the feed bottle was deoxygenated by bubbling N_2(g) to avoid nZVI oxidation and sonicated (at 10,000 rpm) by means of a IKA Ultra-Turrax® T18 sonicator to reduce aggregation of the nZVI particles. Pumping of feed groundwater, which was unaltered during the nZVI pulse, was maintained until the end of the experiment on day 65. Finally, a tracer test was conducted in each column with NaCl (5320 μS/cm) pumped at 4.00 mL/min to determine their porosity (quantified at 0.20–0.22 for all columns).

2.4. Sampling and analysis

Effluent samples were periodically taken throughout the experiment for analysis of pH, NO_3^-, NO_2^-, NH_4^+, Fe, acetate and pesticides (dieldrin and lindane). pH was measured using a pH-meter connected to a pH electrode (Crison GLP-22). The N-containing ions were analyzed by ionic chromatography (IC) (Dionex, ICS-1000) coupled to cationic and anionic detectors (ICS-1000 y ICS-1100, respectively) and controlled by software Chromeleon®chromatographic. Fe was determined by inductively coupled plasma optical emission spectrometry (ICP-OES) (PerkinElmer, Optima 8300). Acetate was analyzed by ionic chromatography (IC) (Dionex, Aquion) equipped with an IonPac AS11-HC column. Pesticides dieldrin and lindane were analyzed by gas chromatography-mass spectrometry (GC-MS) by the certified laboratory IPROMA-Eurofins according to León et al. (2003, 2006). All samples were acidified with HCl and filtered (through Nylon syringe filters 0.22 μm), and refrigerated until needed for analysis. The quality assurance/quality control (QA/QC) protocol comprised the calibration of the instruments with five standards covering the range of the experimental concentrations before

each use. Furthermore, one set of standards, one blank and one duplicate sample were analyzed after every 15 experimental samples. During the tracer test, conductivity was measured with a conductivity meter (Crison GLP 22).

After the column experiments were completed, the columns were dismantled and solid material was removed from different sections of the columns and kept under N_2 atmosphere for analysis using a scanning electron microscope (FESEM) equipped with an energy dispersive X-ray (EDS) for elemental analysis (JEOL JSM 7001-F). Samples were mounted on Cu stubs using a double-sided adhesive carbon tape and sputter-coated with a thin layer of Pt/Pd 80:20 to render them conductive for FESEM observation.

2.5. Microbiological analysis

Soil samples from the columns were also collected for analysis of 16S rRNA genes and two genes involved in HDN (nitrite reductases *nirS* and *nirK*). Samples were directly stored at −20 °C until further processing. Total DNA was extracted from 250 mg homogenized soil samples using a DNeasy PowerSoil kit (Qiagen) following manufacturer's instructions. DNA quality and integrity was inspected by agarose gel electrophoresis. The presence of denitrifying bacteria was assessed by PCR amplification targeting two genes (*nirK* and *nirS*) encoding for structurally different nitrite reductase enzymes. Gene *nirK* encodes for a nitrite reductase containing copper in the active site, while the enzyme encoded by *nirS* contains heme c and heme d1.

Both nitrite reductase genes were amplified from total DNA extracts using two distinct sets of primers described in the literature (Table 2). PCR amplifications were conducted using GOTaq PCR mix (Promega) in total reaction volumes of 25 μL containing 1 μL of DNA extract and 25 pmol of each primer. Amplification products were examined on 1.5% agarose gels and visualized using a GelDoc apparatus (Biorad). For each target, those primer pairs showing the best amplification efficiencies were selected for quantitative analysis by qPCR.

Quantitative PCR (qPCR) reactions were carried out on an Applied Biosystems StepOnePlus Real-time PCR system using PowerUp Sybr Green Master Mix (Applied Biosystems, CA, USA), 1 μL of DNA extract as template and 4 pmol of each primer. Bacterial 16S rRNA gene was amplified using universal primers 341F-518R, while *nirK* and *nirS* genes were amplified using primer pairs nirK583F-nirK909R and nirScd3af-nirSR3cd, respectively. For quantification, 6-point 10-fold standard plasmid dilution series were used. Standard plasmids were obtained by cloning PCR amplification products with pGEM-T Easy Vector System (Promega, WI, USA). Plasmids were purified with the GeneJET Plasmid Miniprep Kit (Thermo Scientific, USA), quantified using Qubit and validated by sequencing.

3. Results and discussion

3.1. Effect of acetate and/or inoculum and/or nZVI on the removal of NO_3^-

Fig. 3 shows the changes in concentrations of NO_3^- (a) and NO_2^- (b) for the five columns before, during, and after the injection of nZVI (on day 48) to Columns A, D, and E. Fig. 3 zooms in from day 27 to better visualize changes produced by the nZVI pulse.

3.1.1. Columns performance before the pulse of nZVI

Columns A and D (both under acetate-free conditions) did not show any noticeable removal of NO_3^-, indicating that the original soil, if not subjected to biostimulation, was not able to promote HDN (although some denitrification was observed for Column A from day 43). In contrast, columns biostimulated with acetate (Column B) and additionally inoculated (Columns C and E) achieved a total removal of NO_3^- (>97%) soon after the beginning of the experiment as described by reaction 1 (note that the results of Column C are not visible in Fig. 3 because they are covered by results of Columns C and E). This behaviour made evident that HDN in the original soil was limited by the absence of a degradable carbon source (as it is commonly the case in aquifers) and that the external addition of acetate yielded a sustainable HDN. The potential of acetate in promoting HDN have been recognised by many studies (Calderer et al., 2010 and references therein). Given the good performance of Column B (supplemented with only acetate) in removing NO_3^-, initial inoculation of aquifer soil (as carried out in Column C) could be considered unnecessary for successful NO_3^- removal. A visual evidence of the proliferation of bacteria in Columns B, C, and E was the appearance of dark spots in the column fillings, typical of the formation of biofilms, in contrast with Columns A and D, for which no change of color was observed.

With regard to the N reduced species (NO_2^- and NH_4^+), NO_2^- was generally detected at levels <2 mg/L (which is below the guideline of 3 mg/L set by the WHO, 2003) for all columns. For Column B a temporary peak of NO_2^- in the effluent (of 15 mg/L) was observed on day 41. This concentration, low in comparison with the NO_3^- removed, could be related to the addition of the target pesticides in influent feed water on day 40, which might have altered HDN (as discussed below). Concerning NH_4^+, it was found always <2 mg/L for all columns (not shown). This indicated that HDN was the predominant mechanism for NO_3^- removal and that biological dissimilatory nitrate reduction to ammonium (DNRA), which might occur when a high organic carbon content is present (Greenan et al., 2006; Gibert et al., 2008), was marginal.

3.1.2. Columns performance during and after the pulse of nZVI

The injection pulse of nZVI in Columns A, D, and E on day 48 resulted in an increase of pH (from influent 7.8 to effluent 8.9–9.2) (not shown). This increase in pH, expected, was explained by the release of OH^- ions during the oxidation of nZVI as described in reaction 3 and was consistent with previous experiments (Gibert et al., 2022).

The injection of nZVI was also accompanied by a sharp drop of the NO_3^- concentration in the effluent (Columns A and D), with removal percentages for both columns of 88% (on a concentration basis). NO_3^- reduction took place as described by reaction 2a and/or 2b. Once the pulse ceased after 6.6 h, the effect of nZVI dissipated and NO_3^- concentration in the effluent from Column A gradually rose until it reached the same concentration as in the influent (100 mg/L), which occurred after approx. 18 days after the injection of nZVI. In Column D, for which the pulse of nZVI was followed by the addition of acetate in feed water, NO_3^- concentration in the effluent first tended to rise once the effect of

Table 2
Primers pairs targeting the *nirK* and *nirS* genes used in the PCR screening. Primers marked with an asterisk were selected for quantitative PCR analyses.

Target	Primer name	Sequence	Annealing T (°C)	Amplicon length	Reference
nirK	nirK583F*	TCATGGTGCTGCCGCGKGACGG	64	326 bp	Yan et al. (2003)
	nirK909R*	GAACTTGCCGGTKGCCCAGAC			
	nirK876F	ATYGGCGGVAYGGCGA	61	170 bp	Henry et al. (2004)
	nirK1040R	GCCTCGATCAGRTTRTGGTT			
nirS	nirScd3af*	GTSAACGTSAAGGARACSGG	58	425 bp	Throbäck et al. (2004)
	nirSR3cd*	GASTTCGGRTGSGTCTTGA			
	nirSCd3aF	AACGYSAAGGARACSGG	57	407 bp	Kandeler et al. (2006)
	nirSR3cd	GASTTCGGRTGSGTCTTSAYGAA			

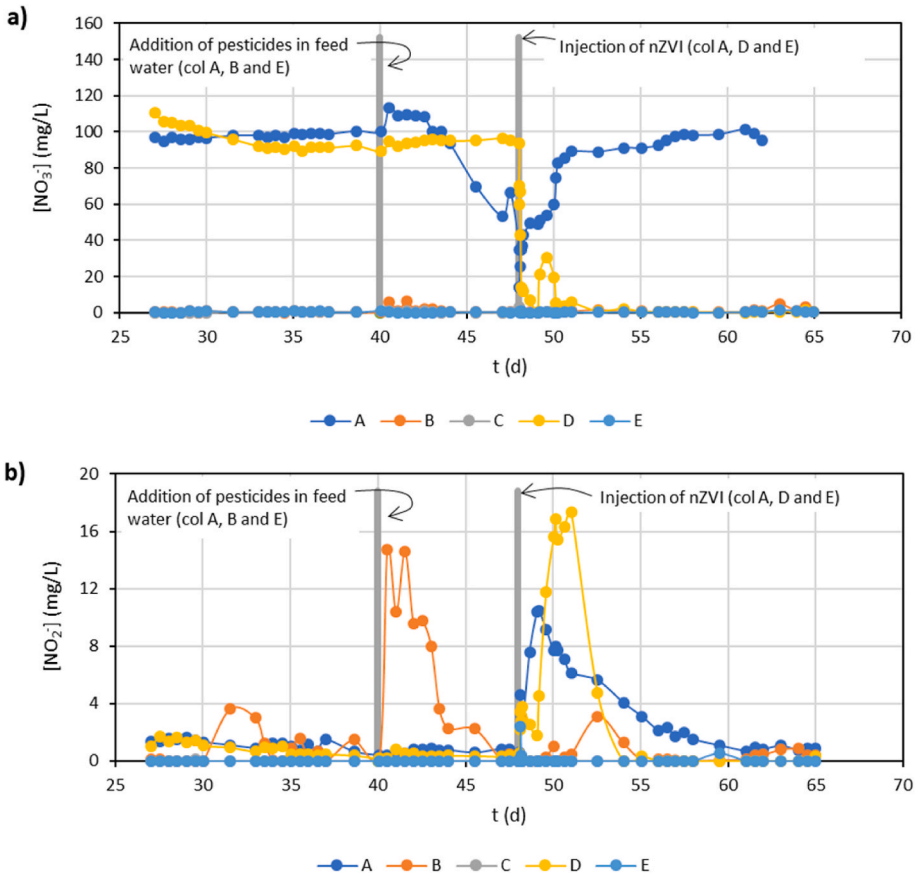

Fig. 3. Variation of the concentration of a) NO_3^- and b) NO_2^- for the five columns. Gray lines represent the addition of pesticides in feed groundwater (for Columns A, B, and E) on day 40 and the injection of nZVI (for Columns A, D, and E) on day 48. Results of Column C are not visible in Fig. 3 because they are covered by results of Columns C and E.

nZVI faded out, but it soon decayed by day 50 to levels below detection limits as HDN rapidly evolved. This fact highlighted that the injection of nZVI did not hinder a fast development of a denitrifying population when acetate was introduced (in other words, that generated Fe^{2+} did not impede that these immediately grew with the addition of acetate). This fact was corroborated by Column E, whose complete NO_3^- removal before the nZVI pulse due to the addition of acetate (biostimulation) was not altered at all by the addition of nZVI on day 48.

With regard to HDN a second observation must be noted: the polymer Tween 80 coating the nZVI did not seem to enhance HDN, as NO_3^- removal was marginal in Column A even though nZVI released a high amount of organic matter once dissolved (e.g. TOC around 50 mg/L according to the composition of the nZVI provided by the manufacturer). The absence of HDN might be due to low biodegradability of Tween 80, at least under the experimental conditions, and/or the lack of a consortium able to degrade this polymer. The scarce studies on biodegradability of Tween 80 as the sole carbon source under anaerobic conditions, performed on batch mode, report that Tween 80 is partially degraded in the order of days, too slowly to be noticed in our column experiments (Yeh and Pavlostathis, 2005; Bretón-Deval et al., 2016).

Temporary NO_2^- formation was observed after the injection of nZVI, with peaks of 11 mg/L (Column A) and 18 mg/L (Column D). These NO_2^- concentrations gradually decreased with time to values below detection limits.

It is worth noting that NH_4^+ was hardly detected in any column (even in those with a strong reduction of NO_3^-). This represented a difference against our previous study in which columns were also subjected to nZVI pulses and a temporary increase of not only NO_2^- but also of NH_4^+ (up to 15 mg/L) through reaction 2 was observed (Gibert et al., 2022). The reason of this difference may lay on the fact that nZVI concentration in the present study (2.3 g/L) was much lower than that in the previous one (10 g/L), which might be more favourable to the reduction of NO_3^- to NH_4^+. If so, this would indicate that NH_4^+ formation can be minimized by controlling the concentration of nZVI. Another possible explanation may lay on the differences in nZVI properties between studies.

3.2. Mass balance on nitrogen species over the column experiments

A mass balance on N-containing species was calculated to determine whether there was a net removal of NO_3^- or only a mere conversion of NO_3^- to NO_2^- and NH_4^+. For this purpose, NO_3^- mass entered with the influent was compared to the total mass of N (ΣN, defined as the sum of masses of $N–NO_3^-$, $N–NO_2^-$ and $N–NH_4^+$) exited with the effluent. Any imbalance between entered NO_3^- mass and exited ΣN would be indicative of a net removal of NO_3^- through the generation of unmonitored N-species (e.g. $N_2(g)$, NO(g), $N_2O(g)$, $NH_3(g)$ …) or through the retention of N-species within the column. The mass of unbalanced N (N_{unb}) was thus calculated by substracting effluent ΣN from the total inlet NO_3^- mass as described equation (5):

$$N_{unb} = q \cdot c^{in}_{NO3-} \cdot t - \int_{t_0}^{t} q \cdot ((c^{eff}_{NO3-} + c^{eff}_{NO2-} + c^{eff}_{NH4+}) \cdot dt \quad (5)$$

where q is the flow rate and the superindexes “in” and “eff” refer to influent and effluent, respectively.

Table 3 summarizes the N-mass balance under each scenario, giving NO_3^- removal, NO_2^- and NH_4^+ formation, and the resulting unbalanced N as percentages with respect to the total mass of NO_3^- entered into the column with the influent.

Table 3
N-mass balance under different column conditions tested in this study (columns described in Fig. 2).

	NO_3^- removal	NO_2^- formation	NH_4^+ formation	Unbalanced N
Unaltered soil conditions[a]	4.7%	3.4%	<1%	1.4%
Under biostimulation[b]	97.5%	7.9%[f]	<1%	89.6%
Under biostimulation + bioaugmentation[c]	91.8%	3.7%	1.5%	87.6%
Under the effect of nZVI[d]	43.4% (99%)[d]	7.1%	<1%	36.4%
Under biostimulation + bioaugmentation + effect of nZVI[e]	>99%	<1%	<1%	>98%

[a] Average values from Columns A and D, both before day 48.
[b] Average values from Columns B.
[c] From Column C.
[d] From Column A considering the period between the pulse of nZVI and the following days (between days 40–50). If only the pulse duration was considered, NO_3^- removal percentage computed increased to >99%.
[e] From Column E between days 40–50.
[f] Mostly in coincidence with target pesticides addition.

As advanced above, under soil original conditions, removal of NO_3^- was marginal (<5%). Under biostimulation (and optionally bioagumentation) conditions HDN was promoted, with a high removal of NO_3^- (>97%), most of it likely being converted into N_2(g) (>87%) following reaction 1. Under the effect of the nZVI pulse, NO_3^- was partially removed (≈43%) over the time comprised from the pulse application and until its effect faded out (between days 40–50) (i.e. until NO_3^- concentration equalled that of the influent). The reduction of NO_3^- followed the ACNR shown in reaction 2. On the other side, NO_2^- formation accounted for approx. 7% of the total entered NO_3^-, NH_4^+ formation for <1% and unbalanced N for approx. 36%. It must be noted that NO_3^- removal percentage computation depends on the time interval under nZVI effect considered. If only the pulse period was considered (i.e. 6.6 h on day 40), NO_3^- removal percentage would be >99%. Under the combined effect of biostimulation, bioaugmentation and nZVI, the NO_3^- was complete (>99%).

Some additional considerations can be drawn on the fate of NO_3^-, NO_2^-, NH_4^+, and unbalanced N. First, besides being reduced, NO_3^- could be adsorbed onto freshly precipitated Fe-(oxy)hydroxides produced by nZVI corrosion (Westerhoff and James, 2003; Tang et al., 2012; Hosseini et al., 2018). Second, NH_4^+ could also be removed via sorption onto Fe-(oxy)hydroxides and/or transformation to NH_3(g) at the attained effluent pH (8.9–9.2), which can strip out from the solution during sampling (Hwang et al., 2011; Tang et al., 2012). Lastly, the unbalanced N (which appears as the major fraction of end-products) may be explained by the production of N_2(g) (Choe et al., 2000; Chen et al., 2005; Yang and Lee, 2005) and/or other unmonitored N gas species (e.g. NO_2, N_2O, N_2H_4). Determination of the relative concentration of these end-products was beyond the scope of this study, but clearly deserves further research.

Concerning the effect of nZVI application and the end-products formed, results of this study showed agreements and discrepancies against published studies. The apparent formation of N_2(g) as end-product agreed with previous studies reporting, from batch experiments, that N_2(g) was the main end-product of ACNR by nZVI in anaerobic conditions and no pH control (Choe et al., 2000; Chen et al., 2005; Zhang et al., 2010a), whereas the main end product when using mZVI was NH_3(g) (Choe et al., 2000). This dependency of N-end products on the size of the ZVI particle (mZVI vs nZVI), which can help interpreted apparently discrepant results between studies, is consistent with other researchers' conclusions. For instance, Westerhoff and James (2003) reported, also from batch experiments, that mZVI favoured the conversion of NO_3^- onto NH_4^+. Other batch studies have reported that the main end-products of ACNR by nZVI in anaerobic conditions and neutral pH were NH_4^+ and N_2(g) with minor NO_2^- formation (Yang and Lee, 2005; Hosseini and Tosco, 2015). Further batch-based studies have reported that NO_2^- and NH_4^+ were the main end-products, but not always the sole ones, formed via ACNR by nZVI with non-relevant N_2(g) formation (Zhang et al., 2010b; Tang et al., 2012; Grau-Martínez et al., 2019). Under continuous flow column experiments in which nZVI was mixed with sand in a packed column, Shubair et al. (2018) observed a >95% removal of NO_3^- (decreasing to 70% after 25 h of experiment and to values between 20 and 40% in the presence of other ions) accompanied by a high generation of NH_4^+ and low formation of NO_2^-. Regarding the scarce published column studies with nZVI pulse-injected like in this one, Hosseini and co-workers evaluated bimetallic nZVI/Cu and reported NO_3^- removal percentages via ACNR in the range of 33–75%, depending on the nZVI dosage (2–8 g/L), NO_3^- concentration (100–300 mg/L) and pore velocity of water (0.125–0.375 mm/s) (Hosseini et al., 2011). It is likely that the higher velocities in the cited study explain (at least partially) why NO_3^- percentage removals were lower than those observed in the present study. Unfortunately, concentration of NO_2^- and NH_4^+ were not reported by the authors. In another nZVI pulse-injected column study, NO_3^- at concentrations of 30 and 78 mg/L was removed by 88–94% through ACNR with nZVI (applied at a dosage of 10 g/L), with NH_4^+ (and NO_2^-) as main end-product (Gibert et al., 2022).

A further considerations must be made concerning the nZVI performance when removing NO_3^-: the composition of groundwater (ionic strength, presence of dissolved ions …) may influence nZVI behaviour (e.g. ionic strength may increase particle aggregation or induce severe Fe dissolution, or dissolved ions may adsorb onto Fe-(oxy)hydroxides), thus altering removal of NO_3^- (Tang et al., 2012; Sun et al., 2017, 2019; Shubair et al., 2018). More research is needed to better understand this influence.

3.3. Evolution of acetate during the column experiments

Fig. 4 shows the evolution of acetate for Columns B, C, D, and E (those receiving acetate continuously or from a certain day) before, during, and after the injection of nZVI (Column A was the only not receiving acetate at any time).

During the first days of experiments (before day 40) the effluent concentration of acetate remained low (<1 mg/L). For Column D this was obviously expected, since this column did not receive acetate before the injection of nZVI. For Columns B, C, and E the reason of these low levels was the consumption of acetate by the HDN reaction, which can be described by equation (6):

$$8\ NO_3^- + 5\ CH_3COO^- + 3\ H^+ \rightarrow 4\ N_2(g) + 10\ HCO_3^- + 4\ H_2O \quad (6)$$

Considering that the applied acetate:NO_3^- ratio (1.06) was higher than the stoichiometric one from reaction 6 (0.625), the low effluent acetate concentration indicated that other processes than HDN were also

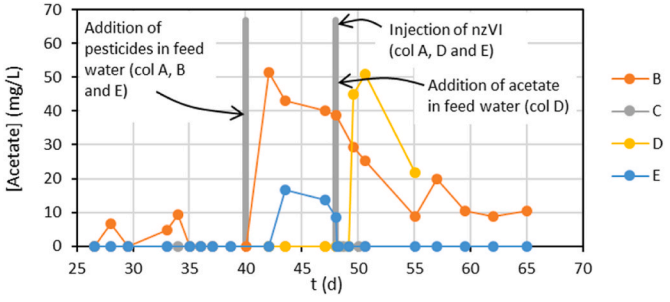

Fig. 4. Evolution of the concentration of acetate during column experiments. Gray lines represent the addition of pesticides in feed groundwater (for Columns A, B, and E) on day 40 and the injection of nZVI (for Columns A, D, and E) on day 48.

contributing to acetate consumption (assimilation for cell growth, oxidation by other heterotrophic microorganisms …) (Calderer et al., 2010).

It is worth noting that for Columns B and E an increment of acetate was observed from day 40 onwards, coinciding with the addition of pesticides in these columns. The fact that this increment was not detected for the column not receiving pesticides (Column D) suggested that the presence of the target pesticides altered, in some way, HDN activity. Temporary inhibitory effects towards HDN activity have been observed for aldrin (closely related to dieldrin) and lindane (Sáez et al., 2006). This temporary weakening of the HDN activity could be behind the peak of NO_2^- observed for Column B also just after day 40 discussed above (Fig. 3b). Over time, the inhibitory effect seemed to disappear, the microbiological activity to resume and, congruently, the concentration of acetate diminished.

For Column D a narrow peak of acetate was observed just after the injection of nZVI, coinciding with the addition of acetate in feed water for this column (Fig. 2). The reason of this peak is that a denitrifying population was still not established (as Column D did not receive acetate until after the nZVI pulse). The narrowness of the peak would indicate that acetate was immediately consumed after the nZVI pulse ceased, i.e. that nZVI did not hinder the development of a denitrifying population once acetate was supplemented. This finding is coherent with the removal of NO_3^- in Column D after the nZVI pulse commented above.

3.4. Removal of pesticides dieldrin and lindane during the column experiments

From day 40 onwards pesticides dieldrin and lindane were added in feed water for Columns A, B, and E until the end of the experiment. Once analyzed, the concentration of dieldrin in feed water was 2.2 μg/L, 1.4 μg/L, and 1.0 μg/L and that of lindane of 2.9 μg/L, 2.2 μg/L, and 2.8 μg/L for Columns A, B, and E, respectively. The estimated mass of dieldrin and lindane entered into each column during the experiments averaged 34.5 μg and 59.2 μg, respectively. Fig. 5 shows the concentration of pesticides in effluents from Columns A, B, and E.

Pesticides dieldrin and lindane exhibited different behaviours. Dieldrin was well removed in all columns and at all times and operation conditions (with and without nZVI) with an average removal >93% (with an averaged removed mass of 32.2 μg per column). By comparing Columns A, B, and E it can be concluded that the removal was not due to biological processes, which was consistent with the refractory character of dieldrin towards biodegradation reported in the bibliography (Chiu et al., 2005). Instead, removal of dieldrin was likely due to adsorption onto soil, according to published studies that document that dieldrin is one of the pesticides that have a larger adsorption coefficient onto soils (Kd) (Weber et al., 2004).

Lindane showed removal percentages noticeably lower in the absence of nZVI (average 38%). Again, a comparison between Columns A, B, and E permitted to conclude that biodegradation did not significantly contribute to lindane removal, also in consonance with the reported poor biodegradability of lindane (Raimondo et al., 2019), and that the moderate removal was due to adsorption onto soil. Though lower than dieldrin, lindane also presents a relatively high adsorption coefficient (Kd) in comparison with most pesticides (Weber et al., 2004). The average mass of lindane adsorbed on the soil was 13.2 μg per column. The hypothesis that lindane removal occurred via adsorption is consistent with the decreasing removal percentage with time, which would be indicative of a gradual saturation of the soil.

The injection of nZVI in columns A and E resulted in a clear increase of the lindane removal up to >91% (although for Column A removal decreased with time). The average mass of lindane retained in the presence of nZVI was 31.4 μg per column. The mechanism of this removal could be chemical degradation by nZVI (Elliott et al., 2009; Abbas et al., 2021) and/or adsorption onto Fe-(oxy)hydroxides formed on nZVI particles (Gusain et al., 2019).

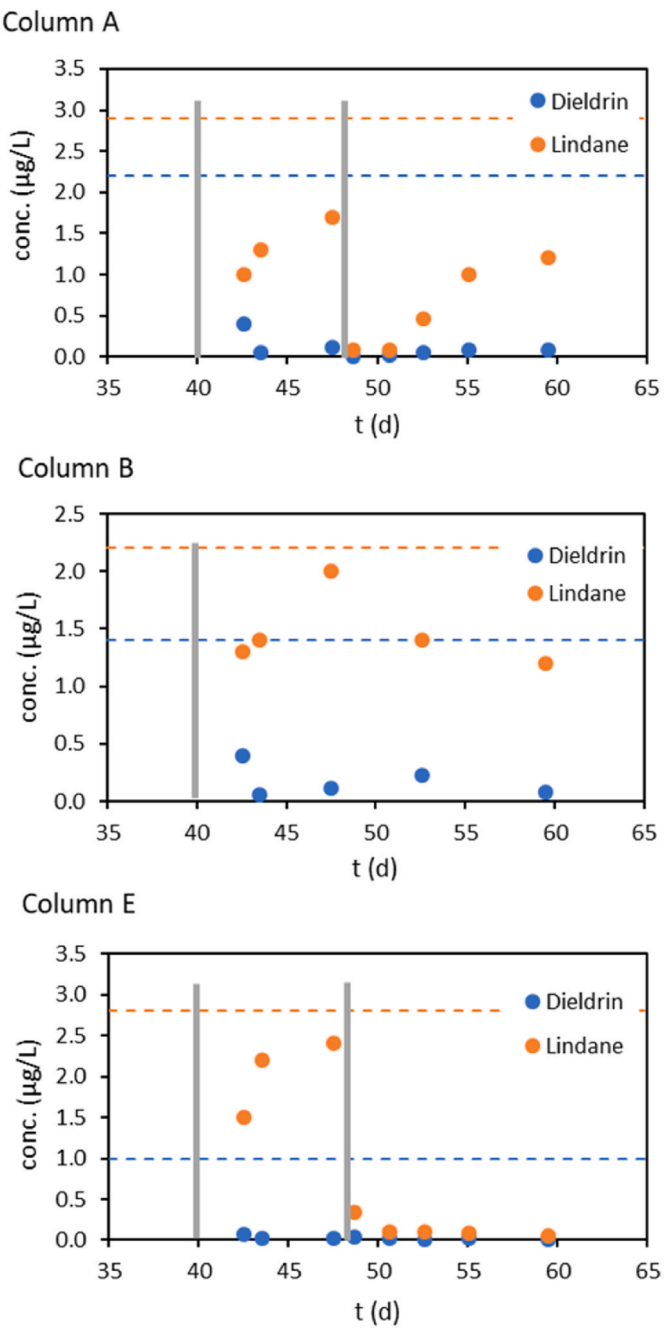

Fig. 5. Evolution of the concentration of pesticides dieldrin and lindane for Columns A, B, and E. Dashed horizontal lines represent the influent concentrations for dieldrin (blue) and lindane (orange). Gray lines represent the addition of pesticides in feed groundwater (for Columns A, B, and E) on day 40 and the injection of nZVI (for Columns A and E) on day 48. (For interpretation of the references to color in this figure legend, the reader is referred to the Web version of this article.)

An issue that deserves mention is the possibility of temporal mobilization of soil fines (and of pesticides adsorbed on them) with the increased flow rates during nZVI injection. As described in Methodology, prior to the experiments water was passed through the columns to remove fines, so it was not expected that large amount of fines prone to be mobilized were still present in the columns. However, mobilization of fines favoured by changes in groundwater flow rate must be taken into account in field applications. Mobilization of pesticides by the organic polymer Tween 80 did not seem to occur either, as concentration of pesticides were not found to be higher in the presence of nZVI (and

therefore Tween 80) (Columns A and E) than in its absence (Column B).

3.5. Microbiological analysis of columns materials

Fig. 6 shows the copy number of ARNr 16S gene (a), *nirS* gene (b) and *nirK* gene (c) in soil material from all Columns A-E collected at the end of the experiment. Blue and orange bars depict the values for samples from the bottom and top of the columns, respectively.

The abundance of genes, particularly those involved in N-transformation processes, was positively related to the NO_3^- removal by HDN throughout the experimental period discussed above.

Column A (under acetate-free conditions over the experiment and with unobserved HDN) clearly exhibited the lowest numbers of gens. Copy numbers of ARNr 16S, *nirS* and *nirK* genes were $1.06{\cdot}10^8$, $1.20{\cdot}10^5$ and $7.49{\cdot}10^3$ copies/g of soil, respectively (without remarkable differences between the bottom and top of the column).

The addition of acetate (biostimulation) applied in Columns B and C boosted the copy numbers of ARNr 16S, *nirS* and *nirK* genes in a similar manner, with number increases by averaged 56, 269, and 282 fold, respectively, confirming that biostimulation was the major driving force

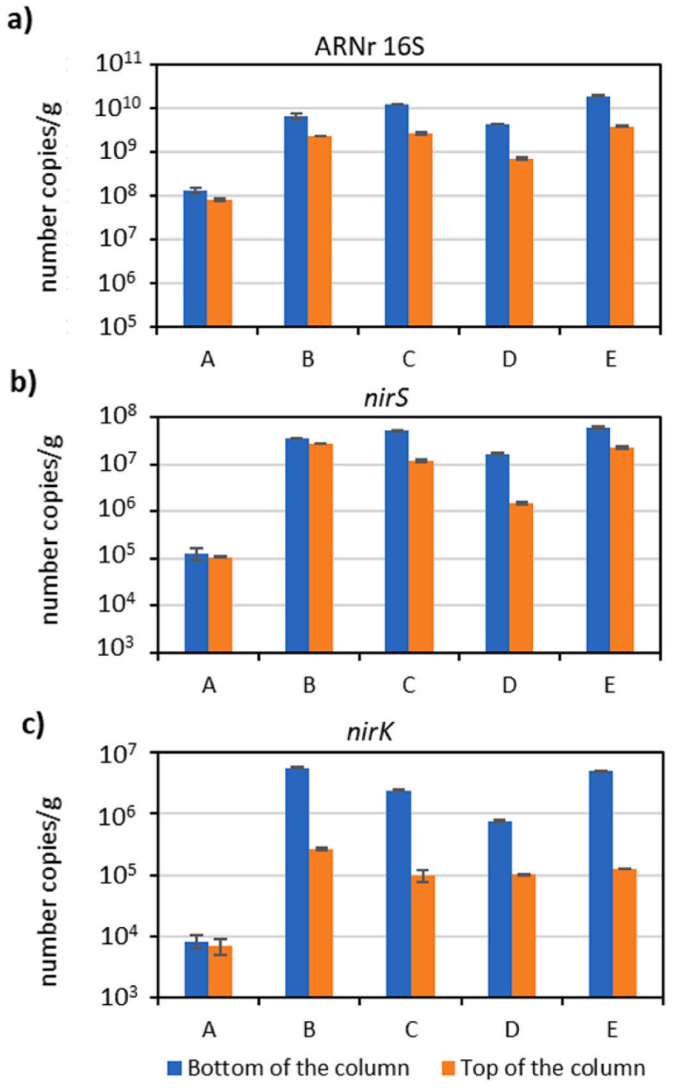

Fig. 6. Quantification of a) ARNr 16S gene, b) *nirS* gene and c) *nirK* gene for all columns material. Blue and orange bars depict copy numbers for samples collected at the end of the experiment from the bottom and top of the columns, respectively. (For interpretation of the references to color in this figure legend, the reader is referred to the Web version of this article.)

in promoting HDN. This also indicated that, on the contrary, initial soil inoculation (bioaugmentation) did not seem to have any influence on microbial abundance developed in columns, as density of non-inoculated Column B and inoculated Column C were of the same order of magnitude. For Column D, which received acetate only from day 48 onwards, the increase of the copy numbers of all genes was less pronounced (increases by 23, 78, and 58 fold, respectively), confirming that the supplementation of acetate was the larger contributor in stimulating HDN.

The effect of the nZVI-pulse on the microbial development can be elucidated by comparing Columns C and E, which were operated exactly under the same conditions but one without receiving nZVI (Column C) and the other receiving nZVI (Column E). It was found that densities of ARNr 16S, *nirS* and *nirK* genes were respectively 34%, 51%, and 23% higher in Column E than in Column C, suggesting that the nZVI-pulse had a beneficial effect that favoured the growth of the microbial population. This enhancement was likely due to the promotion of more reducing conditions (resulting from Fe^0 oxidation as observed in Gibert et al., 2022) favourable for anaerobic denitrifying bacteria. A second observation to be drawn, consistent with this, is that application of a nZVI pulse did not inhibit the growth of the microbial population when followed by a supplementing of acetate (Column D).

With regard to the spatial profile, it was found that abundance of genes was always higher in the bottom of the columns than in the top, especially in Columns B-E (differences higher than 60%). It can be presumed that this was due to the higher concentration of acetate at the inlet zone (i.e. more favourable conditions for HDN to evolve).

Lastly, it must be noted with regard to the relative abundance of the copy numbers of *nirS*-denitrifiers was generally one or two orders of magnitude higher than that of *nirK*-denitrifiers. Predominance of *nirS* over *nirK* genes have been reported in natural environments (Ligi et al., 2014) and engineered systems (Nittami et al., 2009).

3.6. Fate of oxidized nZVI in the column experiments

Effluent Fe for columns receiving a nZVI pulse was always found below detection limits (<0.1 mg/L), indicating that >99% of the injected Fe was trapped in the column. This was not surprising, as Fe^0 oxidises through reactions 2 and 3 to Fe^{2+}, which is further oxidized to Fe^{3+} in the presence of residual oxygen to posteriorly precipitate as $Fe(OH)_3(s)$ or other forms of Fe-(oxy)hydroxides. Precipitation of $Fe(OH)_3(s)$ continuously consumed OH^- ions, which maintained effluent pH in the range of 8.9–9.2. The presence of Fe-(oxy)hydroxides was confirmed by FESEM-EDS analysis of solid samples withdrawn from the columns on the completion of the experiment, which detected particles made of Ca, Si, Mg, Al and O originating from common alumina-silicate minerals of soil aquifer and, for Columns A, D, and E also particles constituted basically by Fe and O (coming from the injected nZVI) (Fig. 7). It is worthnoting that, for columns A, D, and E Fe was detected for solid samples withdrawn from the bottom of the column (and not from the top of it), indicating that Fe was mainly trap in the first 10 cm of the column. Considering that lindane was (partially) adsorbed onto Fe-(oxy)hydroxides formed on nZVI particles, and that nZVI particles were trapped mostly at the bottom of the column, it is expected that more lindane will be found in this part of the column.

4. Conclusions and future perspectives

Results showed that total NO_3^- removal (>97%) could be achieved by either bioestimulation with acetate (removing NO_3^- via HDN) or by injecting nZVI (removing NO_3^- via ACNR). With HDN, NO_3^- was mainly removed through conversion to $N_2(g)$, while with ACNR, NO_3^- was partially converted to $N_2(g)$ and to a lower extent NO_2^-. In the presence of nZVI, unreacted NO_3^- was likely adsorbed onto Fe-(oxy)hydroxide. Combination of both HDN and ACNR resulted also in high (>99%) NO_3^- removal. This is relevant in groundwater remediation as both processes

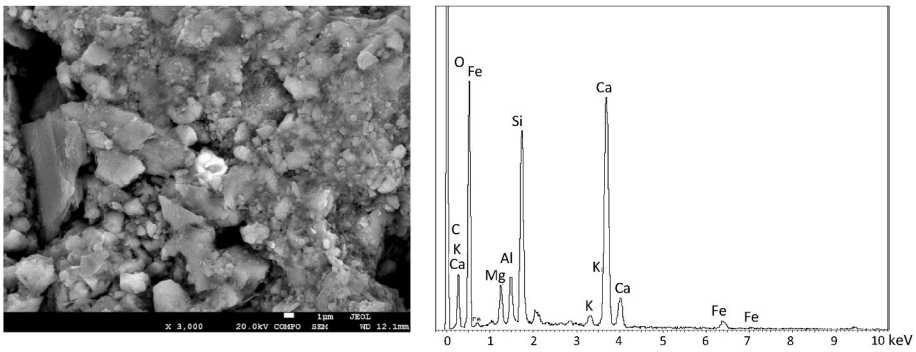

Fig. 7. FESEM-EDS analysis of samples withdrawn from Column D material.

can be alterned or combined to take advantage of the benefits of each individual process while overcoming their disadvantages (e.g. slowness of the process, especially at low temperature, and possible excessive production of biomass for HDN, and excessive formation of NO_2^- and NH_4^+ for ACNR). It is important to note that nZVI did not hinder the evolution of a denitrifying community when acetate was delivered, indicating that nZVI did not pose any persistent toxic effect. It is also worthnoting that the carbon released by the polymer Tween 80 (coating the nZVI used in this study) did not promote HDN, probably because of its poor biodegradability (at least under the experimental conditions). With regard to the target pesticides, the removal was high for dieldrin (>93%) and moderate for lindane (38%), and it was not due to biodegradation but to adsorption onto soil. When nZVI was applied, the removal increased (generally >91%) due to chemical degradation by nZVI and/or adsorption onto formed Fe-(oxy)hydroxides. This permitted to conclude that combination of HDN and ACNR by nZVI can be a useful approach in a WDB system for the simultaneous removal of NO_3^- and pesticides from contaminated groundwater. Moreover, an advantage of injecting the necessary reagents (acetate and nZVI) through a WDB system in comparison with common PRB configurations is that the doses injected can be more easily adapted to variations in composition and flow direction of groundwater over time.

Further efforts to enhance the removal of NO_3^- and pesticides through combined HDN and ACNR and help successful implementation of WDB systems at field-scale should be oriented, for example, to quantify the unmonitored species possibly generated during NO_3^- removal, to synthesize new nZVIs more selective towards the reduction of NO_3^- to $N_s(g)$, (e.g. incorporating noble metals, although this would increase cost of nZVI), to assess alternative organic stabilizers of nZVI more efficient in promoting HDN, to identify interferences posed by coexisting ions on the nZVI performance, to identify the environmental implications of applying the approach proposed in this study (e.g. changes in groundwater pH caused by nZVI oxidation, reductions in soil permeability caused by sedimentation of nZVI into the aquifer, emissions of intermediate $N_2O(g)$ –a powerful greenhouse gas- to the atmosphere caused by incomplete HDN …) and to test nZVI at field-scale applications under real environmental conditions, which are difficult to replicate in laboratory experiments. With regard to the latter, a critical issue that would require especial attention is the control of the growth of biomass near the injection wells for a successful bioremediation of the contaminated groundwater.

CRediT authorship contribution statement

O. Gibert: Conceptualization, Methodology, Resources, Investigation, Visualization, Result interpretation, Writing - original draft; **D. Sánchez:** Conceptualization, Methodology, Investigation, Project administration, Funding acquisition, Writing - reviewer & editing; **J.L. Cortina:** Conceptualization, Validation, Writing - reviewer & editing.

Declaration of competing interest

The authors declare that they have no known competing financial interests or personal relationships that could have appeared to influence the work reported in this paper.

Data availability

The authors do not have permission to share data.

Acknowledgements

This study was funded by Cetaqua through the FeNLAB-BIO project. Financial support was also received through the projects NANOREMOV (CGL2017-87216-C4-3-R) and W4V (PID2020-114401RB-C21 and PID2020-114401RB-C22) from the Spanish MINECO and MICINN, respectively, and from the Catalan AGAUR Agency through the Research Groups Support program (2017-SGR-312). The authors acknowledge the OpenInnovation-Research Translation and Applied Knowledge Exchange in Practice through University-Industry-Cooperation (OpenInnoTrain), Grant agreement number (GAN): 823971, H2020-MSCA-RISE-2018-823971. Finally, they also thank A. Castanyer for his laboratory assistance and M. Grifoll and J. Vila for their help with the microbiological analysis.

References

Abbas, T., Wadhawan, T., Khan, A., McEvoy, J., Khan, E., 2021. Iron turning waste: low cost and sustainable permeable reactive barrier media for remediating dieldrin, endrin, DDT and lindane in groundwater. Environ. Pollut. 289, 117825 https://doi.org/10.1016/j.envpol.2021.117825.

Anderson, E.L., Jang, J., Venterea, R.T., Feyereisen, G.W., Ishii, S., 2020. Isolation and characterization of denitrifiers from woodchip bioreactors for bioaugmentation application. J. Appl. Microbiol. 129, 590–600. https://doi.org/10.1111/jam.14655.

Araújo, R., Castro, A.C.M., Baptista, J.S., Fiúza, A., 2016. Nanosized iron based permeable reactive barriers for nitrate removal - systematic review. Phys. Chem. Earth 94, 29–34. https://doi.org/10.1016/j.pce.2015.11.007.

Banzhaf, S., Nödler, K., Licha, T., Krein, A., Scheytt, T., 2012. Redox-sensitivity and mobility of selected pharmaceutical compounds in a low flow column experiment. Sci. Total Environ. 438, 113–121. https://doi.org/10.1016/j.scitotenv.2012.08.041.

Bretón-Deval, L., Rios-Leal, E., Poggi-Varaldo, H.M., Ponce-Noyola, T., 2016. Biodegradability of nonionic surfactant used in the remediation of groundwaters polluted with PCE. Water Environ. Res. 88, 2159–2168. https://doi:10.2175/106143016X14733681695564.

Burbery, L., Abraham, P., Sutton, R., Close, M., 2022. Evaluation of pollution swapping phenomena from a woodchip denitrification wall targetting removal of nitrate in a shallow gravel aquifer. Sci. Total Environ. 820, 153194 https://doi.org/10.1016/j.scitotenv.2022.153194.

Calderer, M., Gibert, O., Martí, V., Rovira, M., de Pablo, J., Jordana, S., Duro, L., Guimerà, J., Bruno, J., 2010. Denitrification in presence of acetate and glucose for bioremediation of nitrate-contaminated groundwater. Environ. Technol. 31, 799–814. https://doi.org/10.1080/09593331003667741.

Capodici, M., Avona, A., Laudicina, V.A., Viviani, G., 2018. Biological groundwater denitrification systems: lab-scale trials aimed at nitrous oxide production and emission assessment. Sci. Total Environ. 630, 462–468. https://doi.org/10.1016/j.scitotenv.2018.02.260.

Chen, Y.M., Li, C.W., Chen, S.S., 2005. Fluidized zero valent iron bed reactor for nitrate removal. Chemosphere 59, 753–759. https://doi:10.1016/j.chemosphere.2004.11.020.

Chiu, T.C., Yen, J.H., Hsieh, Y.N., Wang, Y.S., 2005. Reductive transformation of dieldrin under anaerobic sediment culture. Chemosphere 60, 1182–1189. http://doi:10.1016/j.chemosphere.2005.02.018.

Choe, S., Chang, Y.Y., Hwang, K.Y., Khim, J., 2000. Kinetics of reductive denitrification by nanoscale zerovalent iron. Chemosphere 41, 1307–1311. https://doi.org/10.1016/S0045-6535(99)00506-8.

Cojean, A.N.Y., Lehmann, M.F., Robertson, E.K., Thamdrup, B., Zopfi, J., 2020. Controls of H_2S, Fe^{2+}, and Mn^{2+} on microbial NO_3-reducing processes in sediments of an eutrophic lake. Front. Microbiol. 11, 1158. https://doi:10.3389/fmicb.2020.01158.

Costa, D.D., Gomes, A.A., Fernandes, M., Lopes da Costa Bortoluzzi, R., Magalhães, M.L. B., Skoronski, E., 2018. Using natural biomass microorganisms for drinking water denitrification. J. Environ. Manag. 217, 520–530. https://doi.org/10.1016/j.jenvman.2018.03.120.

El-Temsah, Y.S., Oughton, D.H., Joner, E.J., 2013. Effects of nano-sized zero-valent iron on DDT degradation and residual toxicity in soil: a column experiment. Plant Soil 368, 189–200. https://doi.org/10.1007/s11104-012-1509-8.

Dominguez, C.M., Parchão, J., Rodriguez, S., Lorenzo, D., Romero, A., Santos, A., 2016. Kinetics of lindane dechlorination by zerovalent iron microparticles: effect of different salts and stability study. Ind. Eng. Chem. Res. 55, 12776–12785. https://doi.org/10.1021/acs.iecr.6b03434.

Elliott, D.W., Lien, H.L., Zhang, W.X., 2009. Degradation of lindane by zero-valent iron nanoparticles. J. Environ. Eng. 135, 317–324. https://10.1061/(ASCE)0733-9372(2009)135:5(317).

Gibert, O., Pomierny, S., Rowe, I., Kalin, R.M., 2008. Selection of organic substrates as potential reactive materials for use in a denitrification permeable reactive barrier (PRB). Bioresour. Technol. 99, 7587–7596. https://doi:10.1016/j.biortech.2008.02.012.

Gibert, O., Cortina, J.L., de Pablo, J., Ayora, C., 2013. Performance of a field-scale permeable reactive barrier based on organic substrate and zero-valent iron for in situ remediation of acid mine drainage. Environ. Sci. Pollut. Res. 20, 7854–7862. https://doi.org/10.1007/s11356-013-1507-2.

Gibert, O., Abenza, M., Reig, M., Vecino, X., Sánchez, D., Arnaldos, M., Cortina, J.L., 2022. Removal of nitrate from groundwater by nano-scale zero-valent iron injection pulses in continuous-flow packed soil columns. Sci. Total Environ. 810, 152300 https://doi.org/10.1016/j.scitotenv.2021.152300.

Graça, C.A.L., Mendes, M.A., Teixeira, A.C.S.C., de Velosa, A.C., 2020. Anoxic degradation of chlorpyrifos by zerovalent monometallic and bimetallic particles in solution. Chemosphere 244, 125461. https://doi.org/10.1016/j.chemosphere.2019.125461.

Grau-Martínez, A., Torrentó, C., Carrey, R., Soler, A., Otero, N., 2019. Isotopic evidence of nitrate degradation by a zero-valent iron permeable reactive barrier: batch experiments and a field scale study. J. Hydrol. 570, 69–79. https://doi.org/10.1016/j.jhydrol.2018.12.049.

Greenan, C.M., Moorman, T.B., Kaspar, T.C., Parkin, T.B., Jaynes, D.B., 2006. Comparing carbon substrates for denitrification of subsurface drainage water. J. Environ. Qual. 35, 824–829. https://doi:10.2134/jeq2005.0247.

Gu, B., Watson, D.B., Wu, L., Phillips, D.H., White, D.C., Zhou, J., 2002. Microbiological characteristics in a zero-valent iron reactive barrier. Environ. Monit. Assess. 77, 293–309. https://doi.org/10.1023/A:1016092808563.

Gusain, R., Gupta, K., Joshi, P., Khatri, O.M., 2019. Adsorptive removal and photocatalytic degradation of organic pollutants using metal oxides and their composites: a comprehensive review. Adv. Colloid Interfac. 272, 102009 https://doi.org/10.1016/j.cis.2019.102009.

Han, K., Yoon, J., Yeum, Y., Park, S., Kim, H.K., Kim, M., Chung, H.M., Kwon, S., Yun, S. T., Kim, Y., 2020. Efficacy of in situ well-based denitrification bio-barrier (WDB) remediating high nitrate flux in groundwater near a stock-raising complex. J. Environ. Manag. 258, 110004 https://doi.org/10.1016/j.jenvman.2019.110004.

Hassanpour, B., Geohring, L.D., Klein, A.R., Giri, S., Aristilde, L., Steenhuis, T.S., 2019. Application of denitrifying bioreactors for the removal of atrazine in agricultural drainage water. J. Environ. Manag. 239, 48–56. https://doi.org/10.1016/j.jenvman.2019.03.029.

Henry, S., Baudoin, E., López-Gutiérrez, J.C., Martin-Laurent, F., Brauman, A., Philippot, L., 2004. Quantification of denitrifying bacteria in soils by *nirK* gene targeted real-time PCR. J. Microbiol. Methods 59, 327–335. https://doi:10.1016/j.mimet.2004.07.002.

Hosseini, S.M., Ataie-Ashtiani, B., Kholghi, M., 2011. Nitrate reduction by nano-Fe/Cu particles in packed column. Desalination 276, 214–221. http://doi:10.1016/j.desal.2011.03.051.

Hosseini, S.M., Tosco, T., 2015. Integrating NZVI and carbon substrates in a non-pumping reactive wells array for the remediation of a nitrate contaminated aquifer. J. Contam. Hydrol. 179, 182–195. https://doi.org/10.1016/j.jconhyd.2015.06.006.

Hosseini, S.M., Tosco, T., Ataie-Ashtiani, B., Simmons, C.T., 2018. Non-pumping reactive wells filled with mixing nano and micro zero-valent iron for nitrate removal from groundwater: vertical, horizontal, and slanted wells. J. Contam. Hydrol. 210, 50–64. https://doi.org/10.1016/j.jconhyd.2018.02.006.

Huang, G., Huang, Y., Hu, H., Liu, F., Zhang, Y., Deng, R., 2015. Remediation of nitrate–nitrogen contaminated groundwater using a pilot-scale two-layer heterotrophic–autotrophic denitrification permeable reactive barrier with spongy iron/pine bark. Chemosphere 130, 8–16. https://doi.org/10.1016/j.chemosphere.2015.02.029.

Hwang, Y.H., Kim, D.G., Shin, H.S., 2011. Mechanism study of nitrate reduction by nano zero valent iron. J. Hazard. Mater. 185, 1513–1521. http://doi:10.1016/j.jhazmat.2010.10.078.

Jiang, D., Zeng, G., Huang, D., Chen, M., Zhang, C., Huang, C., Wan, J., 2018. Remediation of contaminated soils by enhanced nanoscale zero valent iron. Environ. Res. 163, 217–227. https://doi.org/10.1016/j.envres.2018.01.030.

Kandeler, E., Deiglmayr, K., Tscherko, D., Bru, D., Philippot, L., 2006. Abundance of narG, nirS, nirK, and nosZ genes of denitrifying bacteria during primary successions of a glacier foreland. Appl. Environ. Microbiol. 72, 5957–5962. https://doi:10.1128/AEM.00439-06.

Kim, H.S., Kim, T., Ahn, J.Y., Hwang, K.Y., Park, J.Y., Lim, T.T., Hwang, I., 2012. Aging characteristics and reactivity of two types of nanoscale zero-valent iron particles (Fe^{BH} and Fe^{H2}) in nitrate reduction. Chem. Eng. J. 197, 16–23. https://doi.org/10.1016/j.cej.2012.05.018.

León, V.M., Álvarez, B., Cobollo, M.A., Muñoz, S., Valor, I., 2003. Analysis of 35 priority semivolatile compounds in water by stir bar sorptive extraction–thermal desorption–gas chromatography–mass spectrometry Part I: method optimisation. J. Chromatogr. A 999, 91–101. https://doi:10.1016/s0021-9673(03)00600-9.

León, V.M., Llorca-Pórcel, J., Álvarez, B., Cobollo, M.A., Muñoz, S., Valor, I., 2006. Analysis of 35 priority semivolatile compounds in water by stir bar sorptive extraction–thermal desorption–gas chromatography–mass spectrometry Part II: method validation. Anal. Chim. Acta 558, 261–266. https://doi:10.1016/j.aca.2005.10.080.

Ligi, T., Truu, T., Truu, J., Nõlvak, H., Kaasik, A., Mitsch, W.J., Mander, Ü., 2014. Effects of soil chemical characteristics and water regime on denitrification genes (*nir*S, *nir*K, and *nos*Z) abundances in a created riverine wetland complex. Ecol. Eng. 72, 47–55. https://doi.org/10.1016/j.ecoleng.2013.07.015.

Liu, S.J., Zhao, Z.Y., Li, J., Wang, J., Qi, Y., 2013. An anaerobic two-layer permeable reactive biobarrier for the remediation of nitrate contaminated groundwater. Water Res. 47, 5977–5985. https://doi.org/10.1016/j.watres.2013.06.028.

Liu, Y., Wang, J., 2019. Reduction of nitrate by zero valent iron (ZVI)-based materials: a review. Sci. Total Environ. 671, 388–403. https://doi.org/10.1016/j.scitotenv.2019.03.317.

Ludwig, R.D., Smyth, D.J.A., Blowes, D.W., Spink, L.E., Wilkin, R.T., Jewett, D.J., Weisener, C.J., 2009. Treatment of arsenic, heavy metals, and acidity using a mixed ZVI-compost PRB. Environ. Sci. Technol. 43, 1970–1976. https://doi.org/10.1021/es802394p.

Ma, Y., Metch, J.W., Vejerano, E.P., Miller, I.J., Leon, E.C., Marr, L.C., Vikesland, P.J., Pruden, A., 2015. Microbial community response of nitrifying sequencing batch reactors to silver, zero-valent iron, titanium dioxide and cerium dioxide nanomaterials. Water Res. 68, 87–97. https://doi.org/10.1016/j.watres.2014.09.008.

Margalef-Marti, R., Carrey, R., Viladés, M., Jubany, I., Vilanova, E., Grau, R., Soler, A., Otero, N., 2019. Use of nitrogen and oxygen isotopes of dissolved nitrate to trace field scale induced denitrification efficiency throughout an in-situ groundwater remediation strategy. Sci. Total Environ. 686, 709–718. https://doi.org/10.1016/j.scitotenv.2019.06.003.

Marican, A., Durán-Lara, E.F., 2018. A review on pesticide removal through different processes. Environ. Sci. Pollut. Res. 25, 2051–2064. https://doi.org/10.1007/s11356-017-0796-2.

Nittami, T., Magura, T., Imai, Y., Matsumoto, K., 2009. Influence of the electron acceptor on nitrite reductase gene (*nir*) diversity in an activated sludge community. J. Biosci. Bioeng. 108, 394–399. https://doi:10.1016/j.jbiosc.2009.05.007.

Pang, Y., Wang, J., 2021. Various electron donors for biological nitrate removal: a review. Sci. Total Environ. 794, 148699 https://doi.org/10.1016/j.scitotenv.2021.148699.

Peng, Y.P., Chen, T.Y., Wu, C.Y., Chang, Y.C., Chen, K.F., 2019. Dispersant modified iron nanoparticles for mobility enhancement and TCE degradation: a comparison study. Environ. Sci. Pollut. Res. 26, 34157–34166. https://doi.org/10.1007/s11356-018-3739-7.

Raimondo, E.E., Aparicio, J.D., Briceño, G.E., Fuentes, M.S., Benimeli, C.S., 2019. Lindane bioremediation in soils of different textural classes by an Actinobacteria consortium. J. Soil Sci. Plant Nutr. 19, 29–41. https://doi.org/10.1007/s42729-018-0003-7.

Richa, A., Touil, S., Fizir, M., 2022. Recent advances in the source identification and remediation techniques of nitrate contaminated groundwater: a review. J. Environ. Manag. 316, 115265 https://doi.org/10.1016/j.jenvman.2022.115265.

Robertson, W.D., Vogan, J.L., Lombardo, P.S., 2008. Nitrate removal rates in a 15-year-old permeable reactive barrier treating septic system nitrate. Ground Water Monit. Rev. 28, 65–72. https://doi.org/10.1111/j.1745-6592.2008.00205.x.

Sáez, F., Pozo, C., Gómez, M.A., Martínez-Toledo, M.V., Rodelas, B., Gónzalez-López, J., 2006. Growth and denitrifying activity of Xanthobacter autotrophicus CECT 7064 in the presence of selected pesticides. Appl. Microbiol. Biotechnol. 71, 563–567 https://doi.10.1007/s00253-005-0182-8.

Shubair, T., Eljamal, O., Khalil, A.M.E., Matsunaga, 2018. Multilayer system of nanoscale zero valent iron and Nano-Fe/Cu particles for nitrate removal in porous media. Separ. Purif. Technol. 193, 242–254. https://doi.org/10.1016/j.seppur.2017.10.069.

Sun, Y., Lei, C., Khan, E., Chen, S.S., Tsang, D.C.W., Ok, Y.S., Lin, D., Fen, Y., Li, X.D., 2017. Nanoscale zero-valent iron for metal/metalloid removal from model hydraulic fracturing wastewater. Chemosphere 176, 315–323. https://doi.org/10.1016/j.chemosphere.2017.02.119.

Sun, Y., Yu, I.K.M., Tsang, D.C.W., Cao, X., Lin, D., Wang, L., Graham, N.J.D., Alessi, D.S., Komárek, M., Ok, Y.S., Feng, Y., Li, X.D., 2019. Multifunctional iron-biochar composites for the removal of potentially toxic elements, inherent cations, and hetero-chloride from hydraulic fracturing wastewater. Environ. Int. 124, 521–532. https://doi.org/10.1016/j.envint.2019.01.047.

Tang, C., Zhang, Z., Sun, X., 2012. Effect of common ions on nitrate removal by zero-valent iron from alkaline soil. J. Hazard. Mater. 231–232, 114–119. https://doi.org/10.1016/j.jhazmat.2012.06.042.

Throbäck, I.N., Enwall, K., Jarvis, A., Hallin, S., 2004. Reassessing PCR primers targeting nirS, nirK and nosZ genes for community surveys of denitrifying bacteria with DGGE. FEMS Microbiol. Ecol. 49, 401–417. https://doi.org/10.1016/j.femsec.2004.04.011.

Wang, Y., Fang, Z., Kang, Y., Tsang, E.P., 2014. Immobilization and phytotoxicity of chromium in contaminated soil remediated by CMC-stabilized nZVI. J. Hazard. Mater. 275, 230–237. https://doi.org/10.1016/j.jhazmat.2014.04.056.

Weber, J.B., Wilkerson, G.G., Reinhardt, C.F., 2004. Calculating pesticide sorption coefficients (Kd) using selected soil properties. Chemosphere 55, 157–166. https://doi:10.1016/j.chemosphere.2003.10.049.

Westerhoff, P., James, J., 2003. Nitrate removal in zero-valent iron packed columns. Water Res. 37, 1818–1830. http://doi:10.1016/S0043-1354(02)00539-0.

WHO-World Health Organization, 2003. Nitrate and nitrite in drinking-water - background document for development of WHO guidelines for drinking-water quality. Available from: https://apps.who.int/iris/handle/10665/75380. (Accessed 4 April 2022).

Wu, D., Shen, Y., Ding, A., Mahmood, Q., Liu, S., Tu, Q., 2013. Effects of nanoscale zero-valent iron particles on biological nitrogen and phosphorus removal and microorganisms in activated sludge. J. Hazard. Mater. 262, 649–655. http://doi:10.1016/j.jhazmat.2013.09.038.

Yabusaki, S., Cantrell, K., Sass, B., Steefel, C., 2001. Multicomponent reactive transport in an in situ zero-valent iron cell. Environ. Sci. Technol. 35, 1493–1503. http://doi:10.1021/es001209f.

Yan, T., Fields, M.W., Wu, L., Zu, Y., Tiedje, J.M., Zhou, J., 2003. Molecular diversity and characterization of nitrite reductase gene fragments (*nirK* and *nirS*) from nitrate- and uranium-contaminated groundwater. Environ. Microbiol. 5, 13–24. https://doi.org/10.1046/j.1462-2920.2003.00393.x.

Yang, G.C.C., Lee, H.L., 2005. Chemical reduction of nitrate by nanosized iron: kinetics and pathways. Water Res. 39, 884–894. http://doi:10.1016/j.watres.2004.11.030.

Yeh, D.H., Pavlostathis, S.G., 2005. Anaerobic biodegradability of Tween surfactants used as a carbon source for the microbial reductive dechlorination of hexachlorobenzene. Water Sci. Technol. 52, 343–349. https://doi:10.2166/wst.2005.0537.

Zhang, Z., Hao, Z., Yang, Y., Zhang, J., Wang, Q., Xu, X., 2010a. Reductive denitrification kinetics of nitrite by zero-valent iron. Desalination 257, 158–162. http://doi:10.1016/j.desal.2010.02.031.

Zhang, J., Hao, Z., Zhang, Z., Yang, Y., Xu, X., 2010b. Kinetics of nitrate reductive denitrification by nanoscale zero-valent iron. Process Saf. Environ. 88, 439–445. https://doi:10.1016/j.psep.2010.06.002.

Zhou, L., Li, Z., Yi, Y., Tsang, E.P., Fang, Z., 2022. Increasing the electron selectivity of nanoscale zero-valent iron in environmental remediation: a review. J. Hazard. Mater. 421, 126709 https://doi.org/10.1016/j.jhazmat.2021.126709.